

PAPER

View Article Online  
View Journal | View Issue



Cite this: *Environ. Sci.: Processes Impacts*, 2022, 24, 794

# Surface properties and rising velocities of pristine and weathered plastic pellets†

Tom Bond,<sup>ID</sup>\*<sup>a</sup> Jack Morton,<sup>a</sup> Zeinab Al-Rekabi,<sup>b</sup> David Cant,<sup>b</sup> Stuart Davidson<sup>ID</sup><sup>b</sup> and Yiwen Pei<sup>ID</sup><sup>b</sup>

This study compared the surface properties and rising velocities of pristine and weathered plastic production pellets, to evaluate impacts of environmental conditions. Rising velocities were measured for 140 weathered pellets collected from a Spanish beach and compared with pristine low-density polyethylene, high-density polyethylene and polypropylene pellets. A subset of 49 weathered pellets were analysed by Fourier-transform infrared spectroscopy (FTIR), with all found to be polyethylene. Experimental rising velocities for the weathered pellets varied widely, from  $(2.36 \pm 0.01) \text{ cm s}^{-1}$  to  $(10.56 \pm 0.26) \text{ cm s}^{-1}$ , with a mean value of  $(5.79 \pm 0.06) \text{ cm s}^{-1}$ . Theoretical rising velocities were consistently higher than experimental velocities for all pellet types: on average 136% of experimental values for weathered pellets. This discrepancy was more distinct for less spherical pellets, which were often more weathered. Flatter pellets often oscillated as they rose, which explains at least some of this finding. Atomic force microscopy (AFM) analysis revealed that the roughness of the pristine and weathered pellets was  $(59 \pm 11) \text{ nm}$ , and  $(74 \pm 26) \text{ nm}$  respectively. X-ray photoelectron spectroscopy (XPS) analysis showed that the proportion of surface oxidised carbon species were 2.3% and 4.0% of the total carbon signal for a pristine and a weathered pellet, respectively; consistent with photochemical reactions changing the surface chemistry of weathered pellets. As determined by density column, weathered pellets had slightly lower experimental densities than pristine pellets. Overall, this study illustrates why it is important that modelling studies on the environmental fate and/or movements of microplastics validate or correct predictions using experimental data.

Received 25th November 2021  
Accepted 14th April 2022

DOI: 10.1039/d1em00495f

rsc.li/espi

## Environmental significance

The environmental fate of plastic litter is impacted by how environmental processing affects characteristics such as size, shape, surface roughness and density. Plastic production pellets, or nurdles, are an abundant type of plastic litter on shorelines worldwide. They make a good choice for studying how weathering affects the environmental behaviour of plastic litter. Weathered plastic pellets collected from a Spanish beach were compared with pristine pellets. Theoretical rising velocities were consistently higher than experimental velocities, particularly for flatter pellets. Weathered pellets had rougher surfaces, lower densities and a higher proportion of oxidised carbon species on their surface than pristine pellets. This study illustrates why theoretical studies on the environmental fate of microplastics should validate predictions using experimental data.

## 1. Introduction

The global challenge posed by plastic litter is now well recognised. Production of plastic resins and fibres was 380 million metric tons per annum in 2015, with a compound annual growth rate of 8% since 1950.<sup>1</sup> Globally, only 18% of plastics waste is recycled, with 24% incinerated and the remaining 58% either landfilled or entering the natural environment as litter.<sup>1</sup>

Much plastic litter occurs in the form of microplastics, typically defined as particles <5 mm in diameter.<sup>2,3</sup> They can have been manufactured in that size range (primary microplastics) or result from the degradation and fragmentation of larger macroplastics (secondary microplastics). Plastic debris in the ocean has been the focus of much research attention,<sup>4</sup> with around half of the floating marine plastic litter found in subtropical gyres.<sup>5</sup> It has been calculated that 96–98% of buoyant macroplastic is stranded on shorelines within one year of release into the marine environment.<sup>6</sup> Plastic debris has also been recorded in some of the remotest places on Earth, such as Arctic sea ice,<sup>7</sup> around Antarctica,<sup>8</sup> as well as in a variety of freshwater environments.<sup>9</sup>

Nearly 700 marine species, including molluscs, crustaceans, fish and seabirds, are known to interact with plastic litter

<sup>a</sup>Department of Civil and Environmental Engineering, University of Surrey, University Campus, Guildford, GU2 7XH, UK. E-mail: t.bond@surrey.ac.uk

<sup>b</sup>Surface Technology Group, National Physical Laboratory, Hampton Road, Teddington, Middlesex, TW11 0LW, UK

† Electronic supplementary information (ESI) available. See <https://doi.org/10.1039/d1em00495f>



through ingestion, entanglement, and/or smothering.<sup>10</sup> Microplastics can sorb persistent organic micropollutants, including pesticides and flame retardants.<sup>2,11</sup> In turn, there is concern that they may act as vectors for transferring hazardous chemicals to other organisms<sup>12</sup> including humans.<sup>13</sup>

Plastics are an attractive choice for a multitude of applications, including food and drink packaging, medicine and construction. This is related to their durability, impermeability and inertness to a range of biological, physical, and chemical degradation pathways. Nonetheless, they do degrade, with much uncertainty surrounding how rapidly this happens in the environment. One recent study estimated that the half-life (conversion of the first 50% of the polymer mass) for high-density polyethylene in the marine environment ranged from 58 years for bottles to 1200 years for pipes.<sup>14</sup>

Most forms of plastics weathering occur at the polymer surface. An oxidised and embrittled surface layer develops, sometimes accompanied by discolouration. Mechanically degraded sites are susceptible to additional weathering. Photochemical reactions are often important, for example, oxidation by ultraviolet radiation is considered the initial and rate-determining step during the environmental degradation of polyethylene.<sup>15</sup> Chemical and physical degradation can eventually lead to the loss of material properties and total disintegration. Abiotic degradation generally precedes biodegradation.<sup>14,15</sup> Weathering of submerged or floating plastic is often much slower than plastic on beaches or other terrestrial environments, as the presence of water suppresses photochemical oxidative degradation.<sup>16,17</sup> Larger pieces of plastic debris exposed to repeated swell/dry cycles, such as on shorelines, are prone to disintegrate into microplastics.<sup>18</sup>

One important type of plastic litter is plastic production pellets (also known as nurdles or resin pellets), which are the base materials for most commercial plastics.<sup>19</sup> They have been reported from beaches as far apart as in Japan, Hawaii, Malta and Lake Ontario, Canada.<sup>9,20–22</sup> and are the most numerous item of plastic litter on many Mediterranean beaches.<sup>21</sup> Trace metals are known to sorb to their surface.<sup>23</sup> Due to their abundance, production pellets make a good choice to investigate how microplastics are affected by weathering.

This is an important research area as the environmental movements and fate of microplastics, as well as their interactions with other pollutants, are linked to polymer physico-chemical characteristics, such as size, density and surface chemical functionality and topography.<sup>9,14,18</sup> While these characteristics are potentially affected by weathering, for example, alteration of the surface properties of plastic pellets may affect the sorption of other pollutants to their surface,<sup>19</sup> the extent of biofouling and particle aggregation, relatively limited research has been undertaken to address this topic. Therefore, the objectives of this study were to compare the rising velocities, surface properties and densities of weathered and pristine plastic production pellets, in order to evaluate how the former were impacted by environmental conditions. This included assessing how well theoretical predictions of rising velocity matched experimental values. While the authors cannot be certain that the pristine and weathered pellets were of the same

type (e.g. manufacturer and size), it was anticipated this comparison would illuminate some generally applicable differences between pristine and weathered pellets.

## 2. Materials and methods

### 2.1 Pellets tested

The weathered pellets were collected from the high tideline of the beach (Platja del Vivers) at Guardamar del Segura, Alicante, Spain on the morning of 20th June 2019. Pristine low-density polyethylene, high-density polyethylene and polypropylene pellets were supplied by Poli Plastic Pellets Ltd (Hawarden, UK). A representative selection of pellets is shown in Fig. 1. Pellets were rinsed in Milli-Q water and stored at room temperature before being tested. A digital micrometer screw gauge (Oxford Precision, Oxford, UK, Part No. OXD-331-501OK) was used to measure the dimensions of each pellet in three distinct axes: the longest, intermediate, and shortest. Selected pellets were cryogenically milled using a SPEX 6875 freezer/mill (SPEX, Metuchen, NJ), as the chemical composition of milled pellets, as determined by X-ray photoelectron spectroscopy (XPS), were compared with pristine and weathered pellets. In order to identify their polymer-type, a random sample of 49 weathered pellets was analysed using Fourier-Transform Infrared spectroscopy (FTIR) (with a Spectrum 2 FTIR Spectrophotometer by PerkinElmer, Waltham, MA). The spectra were compared to those for pristine polyethene and polypropylene pellets. All 49 weathered pellets analysed by FTIR were found to be polyethylene.

### 2.2 Experimental density measurements

The density of a subset of pellets was measured using two complementary techniques, gas pycnometry and density column measurements, in order to provide an indication of the agreement between experimental and literature density values. Gas pycnometry measures the volume of gas displaced by the tested object. This study used a Micromeritics AccuPyc 1340 (Micromeritics, Norcross, GA), which contains two gas chambers, the sample chamber, and the expansion (reference) chamber. The test gas, in this case helium, is admitted into the sample chamber which contains the sample under test. The pressure is measured, and the valve between the sample chamber and the expansion chamber is opened, allowing gas to fill both chambers, before the pressure is measured again. The ratio between the two measured pressures is used to calculate the volume of the sample in the test chamber:

$$V_s = V_c + \frac{V_R}{1 - \frac{P_1}{P_2}} \quad (1)$$

where  $V_s$  is the sample volume,  $V_c$  is the volume of the empty sample chamber,  $V_R$  is the volume of the reference volume,  $P_1$  is the first pressure (of the sample chamber only) and  $P_2$  is the second (lower) pressure after expansion of the gas into the combined volumes of the sample chamber and the reference chamber. The volumes of the reference and sample chambers were calibrated using a reference sample of known volume





Fig. 1 A sample of the weathered (left) and pristine (right) pellets tested.

(density), in this case pure silicon were used to calibrate the chamber volumes. The densities of three weathered polyethylene and one pristine low-density polyethylene pellets were measured by gas pycnometry. The uncertainty for density measurements by gas pycnometry was estimated to be  $\sim \pm 10 \text{ kg m}^{-3}$ , depending on the (total) size of the sample(s) tested.

The densities of three weathered and five pristine low-density polyethylene pellets were also measured using a density column, by immersion in an aqueous solution of propan-2-ol, at  $23^\circ \text{C}$ . The density of the solution was adjusted by adding small amounts of either water or propan-2-ol and mixing until samples were neutrally buoyant. Liquid density was then determined by taking samples from the solution and measuring in a laboratory density meter (DMA 5000, Anton Paar, Graz, Austria). The meter was calibrated using liquid density standards produced by hydrostatic weighing with a typical uncertainty of 1 part in  $10^5$ . Since this method requires samples to be immersed in liquid, two pellets were weighed, immersed in a water/propan-2-ol solution for 90 minutes, dried and reweighed to check for (permanent) absorption. These two pellets absorbed  $10 \text{ }\mu\text{g}$  and  $20 \text{ }\mu\text{g}$  ( $0.04\%$  and  $0.06\%$  of dry sample weight), indicating errors from liquid adsorption during immersion were negligible. The uncertainty for the measurement of the density of the plastic pellets by density column was (conservatively) estimated to be  $\sim \pm 1.5 \text{ kg m}^{-3}$ .

### 2.3 X-ray photoelectron spectroscopy (XPS) analysis

XPS is a method for analysing a material's surface chemistry, including its elemental composition. XPS was carried out using a Axis Ultra spectrometer (Kratos, Manchester, UK) under ultra-high-vacuum conditions. Measurements were performed using a monochromated aluminium X-ray source, operating at  $15 \text{ kV}$ , with a  $5 \text{ mA}$  emission current. The analysis area used was approximately  $700 \text{ }\mu\text{m} \times 300 \text{ }\mu\text{m}$ , with the maximum depth of analysis  $10 \text{ nm}$ . Survey spectra were obtained using a pass energy of  $160 \text{ eV}$ , and high-resolution spectra were acquired at a pass energy of  $20 \text{ eV}$  or  $40 \text{ eV}$ . Charge compensation was performed using a low-energy electron source and optimised on the C 1s peak. All spectra were referenced to the position of the

C 1s C–C component at  $285 \text{ eV}$  on the binding energy scale. Spectra were quantified using the software CasaXPS version 2.3.22, after applying the National Physical Laboratory (NPL) calculated transmission function using previously performed calibrations. Elemental concentrations were determined using NPL's average-matrix relative sensitivity factors (AMRSF's). Prior to XPS analysis, the pristine sample was treated by rinsing three times in Milli-Q water.

### 2.4 Atomic force microscopy (AFM) analysis

AFM is a method for the high-resolution imaging of surfaces. AFM measurements were performed using the Asylum Research Cypher S AFM (Asylum Research, an Oxford Instruments company, Santa Barbara, California). This instrument is regularly calibrated using a traceably calibrated blaze grating for  $x, y$  calibration and traceably calibrated step height standards for  $z$  height calibration. The AFM is equipped with top view optics and operated in a temperature-controlled laboratory, in a separate enclosed system at  $(27.0 \pm 1.0)^\circ \text{C}$ . Utilizing intermittent contact, the height, amplitude and phase images were recorded for all the samples at a rate of  $0.5 \text{ Hz}$ . Scout 350 silicon nitride cantilevers (NuNano, Bristol, UK) were used, with a spring constant of approximately  $42 \text{ N m}^{-1}$ , resonant frequency of  $350 \text{ kHz}$  and a hemispherical probe apex of  $<10 \text{ nm}$ . The height images representative of the topography of the surfaces were post-processed flattened using a first-order plane fit which excluded any artefacts in the images. Both the root mean square (RMS) roughness ( $S_q$ ) and mean roughness ( $S_a$ ) of surface were measured for all images.

### 2.5 Rising velocity measurement in seawater

A test rig was built to measure rising velocity (Fig. 2). This involved a large, upended measuring cylinder suspended over a large tank, filled with artificial seawater. Synthetic seawater was prepared to  $35 \text{ g L}^{-1}$  sea salts in Milli-Q water.<sup>24</sup> To measure the terminal experimental rising velocity, the time taken for a particle to travel between two lines  $39 \text{ cm}$  apart in the upper portion of a  $2 \text{ L}$  measuring cylinder ( $71 \text{ mm}$  diameter and  $51 \text{ cm}$



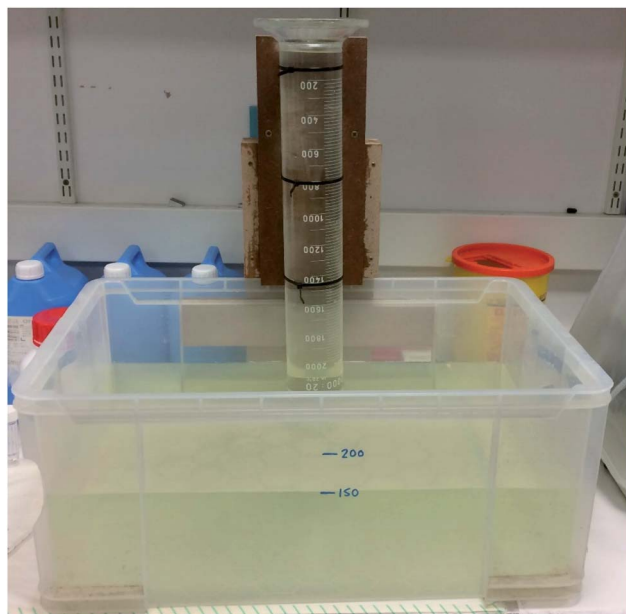


Fig. 2 The test rig for measuring rising velocity.

height) was recorded at room temperature ( $20 \pm 2^\circ\text{C}$ ) using a digital timer, with each pellet released from the same position below the cylinder, with care taken not to introduce turbulence. Velocities were measured after pellets had travelled an accelerating distance of  $>15\text{ cm}$ ,<sup>25</sup> previously considered sufficient for microplastics to reach terminal velocity. The rising velocity of each pellet was measured at least three times, data in the graphs below are the mean values for the three closest values. The movement of pellets along the column was monitored, with outlying values being discounted where abnormal lateral movement caused the pellets to collide with the sides of the column. The standard deviation of the variability between triplicate experimental tests was generally  $<0.12\text{ s}$ . Across all rising velocity experiments, this equates to a mean standard deviation of  $\pm 0.06\text{ cm s}^{-1}$  (or 1.1% of the rising velocity). The rising velocity of 140 weathered pellets, and 20 of each of the three types of pristine pellets, was measured in this way.

## 2.6 Theoretical rising velocities

Theoretical rising velocities of the pellets were calculated using two methods. The first was the approach of Dietrich<sup>26</sup> as previously applied to calculate theoretical settling/rising velocities for microplastics in water.<sup>27–29</sup> Initially the Equivalent Spherical Diameter ( $D_n$ ) of the pellets was calculated, defined by Kowalski and co-workers<sup>27</sup> as:

$$\text{Equivalent spherical diameter } (D_n) = (abc)^{\frac{1}{3}} \quad (2)$$

where,  $a$  is the longest,  $b$  the intermediate and  $c$  the shortest dimension. Subsequently this was used as an input ( $D_n$ ) to calculate the dimensionless particle size ( $D_*$ ):

$$D_* = \frac{(\rho_s - \rho_f)gD_n^3}{\rho_f \nu^2} \quad (3)$$

where  $\rho_s$  is the solid density (variable, depending on pellet type);  $\rho_f$  the fluid density ( $1028\text{ kg m}^{-3}$ );  $g$  the gravitational acceleration ( $9.81\text{ m s}^{-2}$ ) and  $\nu$  the kinematic viscosity of fluid ( $1.06 \times 10^{-6}\text{ m}^2\text{ s}^{-1}$ ). The density of the synthetic seawater was measured experimentally. Pellet density values used were mean values of a range of literature values:<sup>9</sup>  $905\text{ kg m}^{-3}$ ,  $920\text{ kg m}^{-3}$  and  $955\text{ kg m}^{-3}$  for polypropylene, low-density polyethylene and high-density polyethylene, respectively. All the weathered pellets were treated as low-density polyethylene when calculating theoretical rising velocities, since experimental density values for the three weathered pellets tested by density column were closest to this polymer type. Next, the dimensionless settling velocity ( $\omega_*$ ) was calculated using one of the two following equations:

$$\omega_* = 1.74 \times 10^{-4} D_*^2 \text{ for } D_* < 0.05 \quad (4)$$

$$\log(\omega_*) = -3.7615 + 1.92944 \log(D_*) - 0.09815(\log(D_*))^2 - 0.00575(\log(D_*))^3 + 0.00056(\log(D_*))^4 \text{ for } 0.05 \leq D_* \leq 5 \times 10^9 \quad (5)$$

Finally, the rising velocity was calculated using

$$V_r = -\left(\left(\frac{\rho_s - \rho_f}{\rho_f}\right)g\nu\omega_*\right)^{1/3} \quad (6)$$

The Corey Shape Factor used to quantify the shape of each pellet was calculated from the three pellet dimension measurements taken during initial pellet classification:

$$\text{Corey Shape Factor} = \frac{c}{\sqrt{ab}} \quad (7)$$

A particle with a Corey Shape Factor of 0 is a 2-dimensional disc and a particle with a Corey Shape Factor of 1 is a sphere. The Corey Shape Factor has previously been used to evaluate the sphericity of natural particles and how this affects their settling velocities.<sup>26</sup> For comparison, rising velocity was also calculated using the recently developed method of Waldschlager and Schütttrumpf,<sup>30,31</sup> which itself is a modified version of Stokes' Law. Following this method, the first-step is to calculate the Reynold's number ( $\text{Re}$ ):

$$\text{Re} = \frac{V_r D_n}{\nu} \quad (8)$$

Followed by the drag coefficient ( $C_d$ ) for rising particles:

$$C_d = \left(\frac{20}{\text{Re}} + \frac{10}{\text{Re}} + \sqrt{1.195 - \text{CSF}}\right) \left(\frac{6}{P}\right)^{1-\text{CSF}} \quad (9)$$

where  $P$  is the Powers roundness, a scale which ranges from 0 (very angular) to 6 (well rounded). Finally, the theoretical rising velocity was calculated using:

$$V_r = \sqrt{\frac{4}{3}} \frac{D_n}{C_d} \left(\frac{\rho_s - \rho_f}{\rho_f}\right)g \quad (10)$$

In this approach, the experimental rising velocity was used as the initial assumed velocity ( $V_r$ ) in eqn (8) and the values



obtained from eqn (8)–(10) were iteratively adjusted until values for the assumed velocity (in eqn (8)) and calculated velocity (in eqn (10)) converged.

### 3. Results

#### 3.1 Experimental rising velocities of weathered and pristine pellets

Experimental rising velocities for the 140 weathered pellets varied from  $(2.36 \pm 0.01) \text{ cm s}^{-1}$  to  $(10.56 \pm 0.26) \text{ cm s}^{-1}$ , with a mean value of  $(5.79 \pm 0.06) \text{ cm s}^{-1}$  (Fig. 3). Mean rising velocities for pristine low-density polyethylene, high-density

polyethylene and polypropylene pellets were respectively  $(5.31 \pm 0.06) \text{ cm s}^{-1}$ ,  $(6.14 \pm 0.07) \text{ cm s}^{-1}$  and  $(7.42 \pm 0.08) \text{ cm s}^{-1}$  (Fig. 3). For comparison, data reported in the literature show experimental rising velocities for various types of weathered microplastics collected from environmental samples ranged from  $0.18 \text{ cm s}^{-1}$  to  $19.85 \text{ cm s}^{-1}$ , while experimental sinking velocities for differently shaped microplastics sized from  $0.3 \text{ mm}$  to  $3.6 \text{ mm}$  varied from  $0.6 \text{ cm s}^{-1}$  to  $9.1 \text{ cm s}^{-1}$ .<sup>27,31</sup> Both these datasets agree well with the current study. As can be seen from Fig. 3, rising velocities were more variable for the weathered pellets than the other pellet types tested. This pattern is at least partially explained by the weathered pellets having more variable sizes and shapes than the pristine pellets. To illustrate, Corey Shape Factors for the weathered pellets ranged from 0.31–0.97 and for all types of pristine pellets from 0.40–0.82 (Fig. 3). It is interesting that a minor proportion of the weathered pellets were actually more spherical than the pristine pellets (Fig. 3). The respective comparison for Equivalent Spherical Diameter was from  $0.0024 \text{ m}$  to  $0.0046 \text{ m}$  (weathered pellets) and  $0.0033 \text{ m}$  to  $0.0040 \text{ m}$  (all pristine pellets) and for the log of the dimensionless particle size from 4.13–4.94 (weathered pellets) and 4.45–4.82 (all pristine pellets). These differences reflect variability in the manufacturing process, and perhaps the environmental processing, of the weathered pellets. Another likely contributor to the variable rising velocities of weathered pellets is that their density values varied more widely than amongst the pristine pellets.

Meanwhile, Karkanorachaki *et al.*<sup>32</sup> measured the rising velocity of 12 weathered and 12 virgin plastic pellets exposed to the marine environment for 300 days. The rising velocities of virgin and weathered low-density polyethylene, high-density polyethylene and polypropylene pellets varied from  $2.25 \text{ cm s}^{-1}$  to  $3.22 \text{ cm s}^{-1}$ , from  $3.11 \text{ cm s}^{-1}$  to  $6.25 \text{ cm s}^{-1}$  and from  $2.94 \text{ cm s}^{-1}$  to  $3.67 \text{ cm s}^{-1}$  respectively.<sup>32</sup> Thus, the rising velocities reported were overall somewhat lower than in the current study and were likely impacted by the presence of holes inserted in the pellets to pass a wire through.

As expected, there was a general trend for rising velocity to increase with increasing dimensionless particle size ( $D_*$ ), Equivalent Spherical Diameter and Corey Shape Factor (Fig. 3). The dimensionless particle size is the ratio of the gravitational force acting on a particle to the viscous resistance exerted by the fluid, and has been previously deployed to investigate the influence of particle size and density on the settling velocity of natural particles.<sup>26</sup> All the relationships in Fig. 3 are explicable from the fundamental mathematical equations used to calculate theoretical rising velocities described above. More spherical particles will rise or settle more quickly than angular, flat or irregularly shaped particles of similar mass due to the decreased drag or resistance they experience and because they experience less secondary movements. Furthermore, in Fig. 1, it can be seen that the more heavily weathered pellets (which tended to be more discoloured or yellower) were also less spherical. Nonetheless, there were multiple pellets which were exceptions to this pattern (Fig. 3). The yellow colour of weathered pellets such as shown in Fig. 1 is due to weathering, specifically the presence of increased ketone groups as

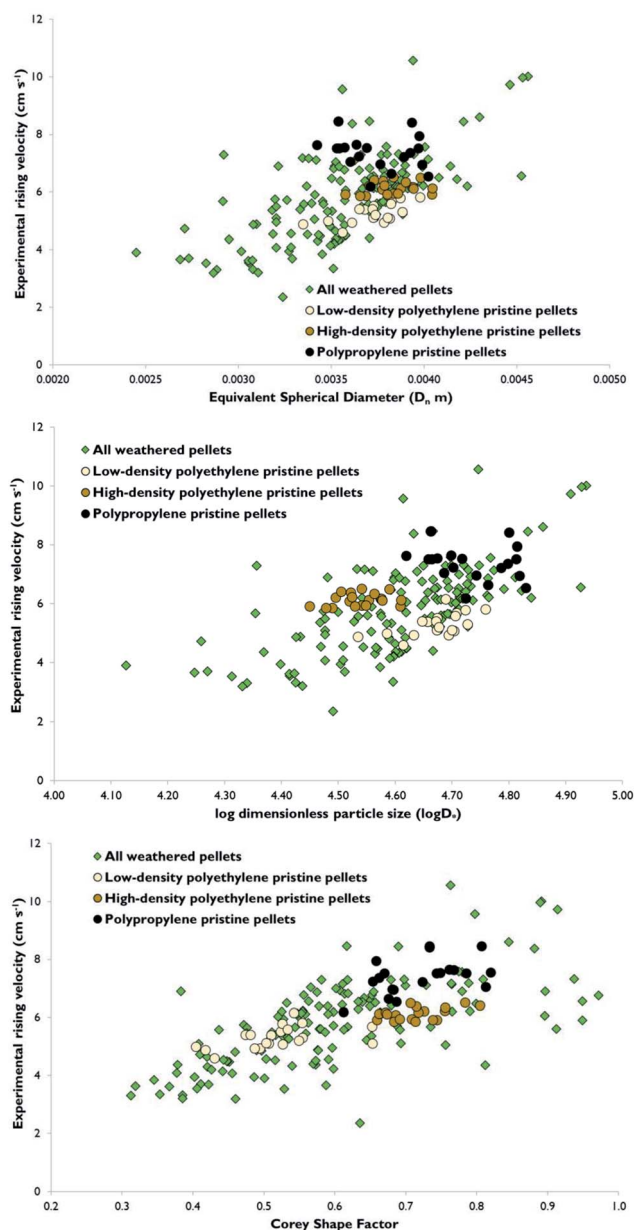


Fig. 3 Relationships between the experimental rising velocity and Equivalent Spherical Diameter ( $D_e$ , top) dimensionless particle size ( $D_*$ , middle), and Corey Shape Factor (bottom). Each data point represents the mean of three replicate measurements.



determined by FT-IR, rather than use of dyes or other additives, with pale yellow indicating less exposure to the marine environment than dark yellow.<sup>19,33</sup>

### 3.2 Theoretical rising velocities

Theoretical rising velocities were calculated using two methods: those of Dietrich<sup>26</sup> and Waldschläger and Schüttrumpf.<sup>30</sup> The latter was found to be more accurate (Fig. 4 and SM-1†). To illustrate, across the total dataset, theoretical rising velocities on average were 151% and 133% of experimental values by the two methods, respectively. As shown by these values, theoretical rising velocities were consistently higher than experimental rising velocities, for all pellet types except the pristine high-density polyethylene pellets calculated by the Waldschläger and Schüttrumpf method (Fig. 4 and SM-1†). For pristine high-density polyethylene pellets, theoretical rising velocities on

average were 107% of experimental values by the Waldschläger and Schüttrumpf method. For weathered pellets, low-density polyethylene pellets and polypropylene pellets, equivalent values were 136%, 140% and 117% (Fig. 4).

Literature density values were used as input values when calculating theoretical rising velocities. Since pellet density was experimentally measured for only a small number of pellets, it is possible that the literature values introduced systematic error into when calculating theoretical rising velocities. However, this does not appear to be the only explanation, since the lower part of Fig. 4 shows that it was mainly pellets with lower Corey Shape Factors which had the highest theoretical rising velocities (Fig. 4). For example, for weathered pellets with a Corey Shape Factor  $\leq 0.45$ , on average theoretical rising velocities were 160% of experimental values, whereas for the remaining pellets, with Corey Shape Factor

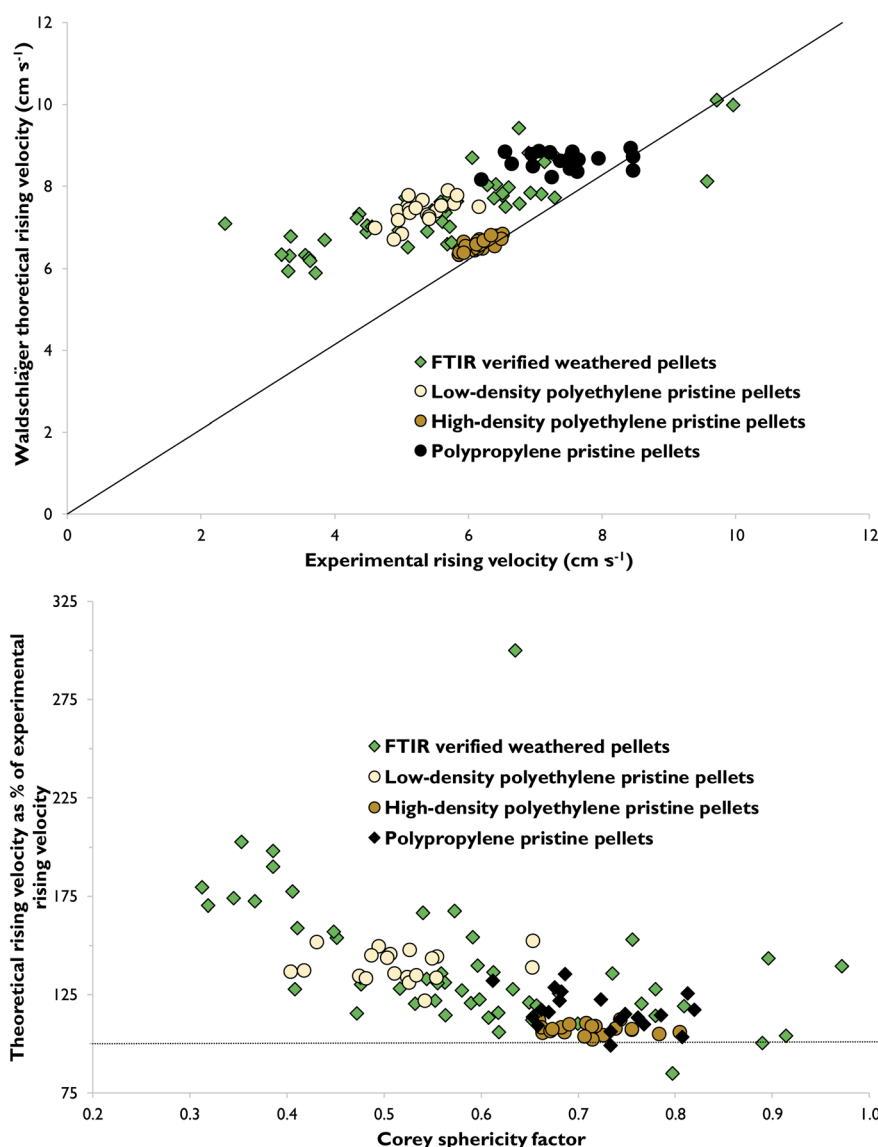


Fig. 4 Relationships between experimental and Waldschläger theoretical rising velocities (top) and between the Corey sphericity factor and Waldschläger theoretical rising velocity as a % of experimental rising velocity.



>0.45, the equivalent value was 130%. Flatter pellets, with lower Corey Shape Factors, were observed to oscillate more frequently, in largely horizontal directions, as they rose through the column. While repeats were performed where pellets collided with the column sides, such movements were generally more widespread in flatter particles. This oscillation led to experimental rising velocities being often slower for flatter pellets. Indeed, a greater number of spherical pellets were observed to move more directly, most likely since they were more streamlined. The small number of weathered pellets with theoretical rising velocities which were lower than experimental values were all relatively spherical pellets (Fig. 4).

### 3.3 Surface properties of weathered and pristine pellets

Comparative analysis by AFM demonstrated that the roughness of the different pellet types increased in the order pristine  $\leq$  weathered (Table SM-1†). This applied to both mean roughness ( $S_a$ ) and root mean square roughness ( $S_q$ ). To illustrate, based on  $S_a$  values from seven different locations in each sample, the roughness of the pristine, and weathered pellets was ( $59 \pm 11$ ) nm and ( $74 \pm 26$ ) nm respectively (Table SM-1†). However, while the average roughness of weathered pellets was higher than pristine pellets, differences were within experimental error and there were no observed significant differences in either  $S_a$  and  $S_q$  between these two types of pellets, defined as  $P < 0.05$ , as determined using a Student's  $t$ -test.

These data confirmed what can be seen from visual inspection of the AFM images: that the pristine-milled and weathered samples had rougher surfaces than the pristine pellet sample (Fig. SI-2†). Previously, using scanning electron microscopy (SEM) revealed that virgin pellets had smooth, uniform surfaces, whereas those of weathered pellets were rough and uneven, with higher surface areas.<sup>19</sup> A corresponding pattern was noted with virgin and artificially-weathered polyvinyl chloride (PVC) pellets.<sup>34</sup> Such differences are important, as they may influence the behaviour of the pristine and weathered pellets, e.g. as manifested in distinct rising velocities. As noted above, less spherical (and more heavily weathered/rougher) pellets rose more slowly than expected on the basis of theoretical rising velocities. Differences in the overall pellet shape are accounted for in various ways depending on the method used to calculate theoretical rising velocities. In the current study, the Equivalent Spherical Diameter, Corey Shape Factor and Powers roundness were used to quantify this. However, surface roughness is not included in the relevant equations (see Methods section) and this may be a limitation when they are applied to weathered plastic samples. Given the minor differences in surface roughness between pristine and weathered pellets, this is unlikely to be a major factor driving rising/settling velocities though it perhaps had a minor impact. Interestingly, the rising velocities of low-density polyethylene, high-density polyethylene and polypropylene pellets were essentially unchanged by 300 days' environmental exposure to seawater.<sup>32</sup> This indicates that profound changes to the shape and surface morphology of pellets did not occur under these conditions; such alterations are expected to occur far more quickly to pellets on beaches or

other terrestrial environments rather than submerged or floating plastic.<sup>16</sup>

XPS analysis was used to determine the superficial elemental composition of the different samples (Fig. 5 and Tables SI-1, SI-2†). The pristine-milled sample exhibited a very clean spectrum with only the C 1s peak referenced to a binding energy of 285.0 eV (Fig. 5 and Table SM-3†) which is characteristic for polyethylene; high resolution C 1s spectra were used to quantify the amount of oxidised *versus* non-oxidised carbon in the other samples. Note that previously, polyethylene has been used as a reference material during the intensity calibration of XPS analysis.<sup>35</sup> Higher binding energy 'shoulders' in other samples indicate the presence of trace amounts of oxidised carbon species in the range from  $\sim 286$  eV to  $\sim 289$  eV binding energy (Fig. 5). The functional groups responsible for these shoulders include C–O, C=O and COOH. In the pristine pellets, the proportion of oxidised carbon species, as determined by peak-fitting of the C 1s high-resolution spectrum, was 2.3% of the total carbon signal, or 2.1% of the sampled volume. Corresponding numbers for the weathered pellet were 4.0% and 3.4%, respectively, which are consistent with increase in the O 1s signal in this sample, relative to the other sample types. This pattern can be explained by the surface of the weathered pellets containing more carbonyl and carboxylic acid groups, the presence of which was initiated *via* photochemical oxidation reactions.<sup>9,15</sup> In a previous study based on beached plastic production pellets in Malta it was reported that the degree of yellowing or darkening of pellets was associated with an increase in the carbonyl index (as quantified by FTIR), itself linked to the amount of photochemical oxidation.<sup>21</sup> Darkened or discoloured pellets are evident in Fig. 1 of the current study, many flatter and/or smaller than the pristine pellets, though there are also weathered pellets which are flatter but not noticeably discoloured. Since weathering can occur *via* different pathways, it can be hypothesised that the amount of oxidised carbon species (e.g. as monitored by FTIR or XPS) or yellowing/darkening are proxies for the amount of photochemical oxidation, whereas surface roughness and shape changes, including the production of flatter pellets, relate to physical abrasion. These two weathering processes will often correlate with each other, as beached pellets can be expected to experience both greater photochemical oxidation and physical abrasion, enhanced by repeated swell/dry cycles, relative to those in water.<sup>9</sup>

The presence of small amounts of nitrogen, sodium and calcium in the weathered and pristine pellets with salt can be explained by their exposure to synthetic seawater, as negligible amounts of these elements were present in the pellets which were not exposed to synthetic seawater (Table SM-2†).

### 3.4 Experimental densities of weathered and pristine pellets

In order to verify the theoretical density values used during rising velocity calculations, experimental density values were measured for a subset of pellets (Fig. 6). Pellets tested were either pristine polyethylene pellets or weathered pellets which had been identified as polyethylene using FTIR. In this study



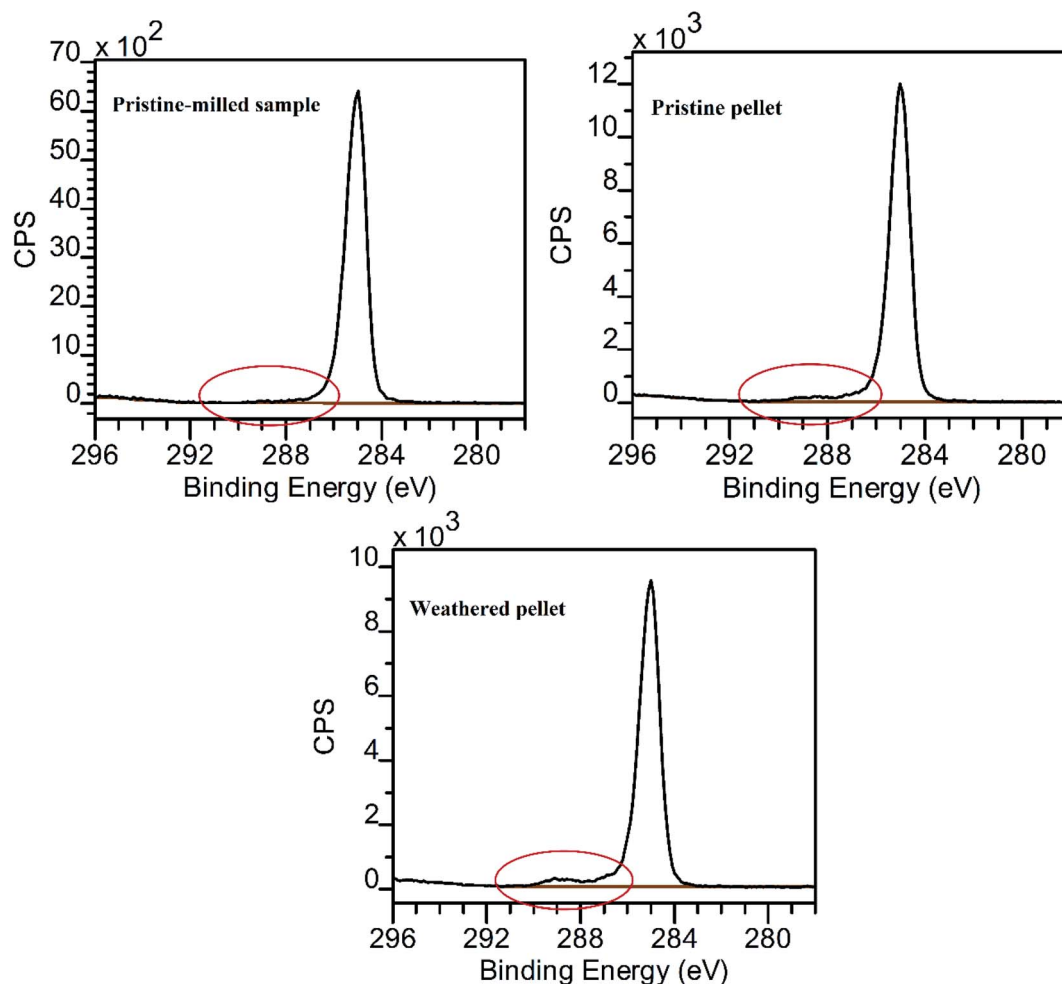


Fig. 5 Differences in the XPS signal related to the presence of oxidised carbon species. CPS = counts per second.

theoretical density values of  $920 \text{ kg m}^{-3}$  and  $955 \text{ kg m}^{-3}$  were used when calculating theoretical rising velocities for low-density and high-density polyethylene pellets, respectively. In Fig. 6, dashed lines at  $910 \text{ kg m}^{-3}$  and  $960 \text{ kg m}^{-3}$  delineate the range of literature values given for low-density and high-density

polyethylene.<sup>9</sup> Given the small sample size, the data in Fig. 6 should be viewed with some caution. Compared to helium pycnometry, density column measurement is a more suitable analytical method for measuring the densities of these pellet samples. It provides density measurements with relatively high

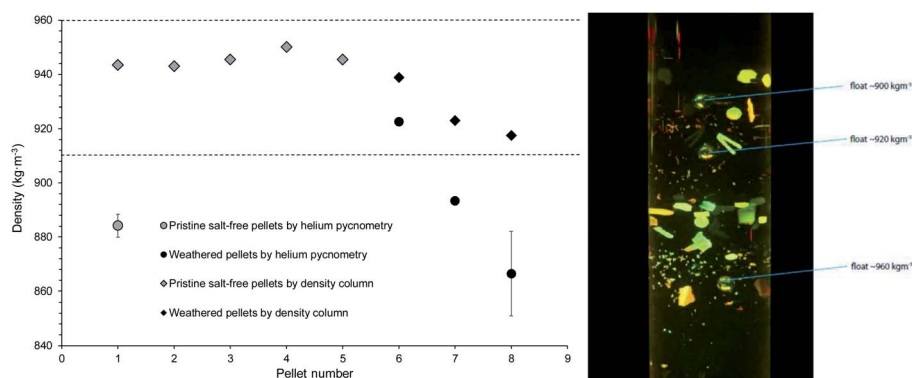


Fig. 6 Experimental verification of pellet density values using helium pycnometer ( $n = 4$ ) and density gradient column ( $n = 8$ ). The horizontal dashed lines in the graph represent limits of literature density values for polyethylene (both low density and high density) (Bond *et al.*, 2018 (ref. 9)). The photo shows the density gradient column in use (courtesy of H&D Fitzgerald).



precision for both the pristine and the weather samples, *e.g.* the relative standard deviations of all samples are within 5% (Fig. 6). The density gradient column performed better in this respect, and this technique appears to be a relatively quick method for measuring the density of plastic particles. Its accuracy was estimated conservatively as being  $\sim \pm 1.5 \text{ kg m}^{-3}$ . Notably, the density of the weathered pellets was slightly less than the pristine pellets, the respective range of values being 918–939  $\text{kg m}^{-3}$  and 943–950  $\text{kg m}^{-3}$  (Fig. 6). Since the initial density of the weathered pellets (*i.e.*, before weathering) is unknown, it is possible that environmental processing did not change pellet density values in this case. Conversely, a more intriguing explanation is that initial density values were similar to those of the pristine pellets in Fig. 6 and became reduced by weathering. There is a precedent for polymer density changing upon degradation in literature; as in a study under controlled laboratory conditions, as degradation proceeded increases in polymer density were observed, presumably associated with changes in chemical composition of the surface layer; subsequently formation of voids reduced density.<sup>36</sup>

## 4. Discussion

One important finding from this study was that weathered pellets had far more variable experimental rising velocities than pristine pellets (Fig. 3). Moreover, with less spherical (*i.e.* typically more heavily weathered pellets) there was a bigger discrepancy between theoretical and experimental rising velocity (the former being lower), so the settling/rising behaviour of flatter (and typically more heavily weathered plastics) were less accurately predicted than more spherical (and typically less weathered samples). All pellets with a Corey Shape Factor  $< 0.4$  were weathered, rather than pristine, pellets. Meanwhile, all pellets with a Corey Shape Factor  $> 0.82$  were weathered pellets, which indicates that beached pellets come in a diverse range of shapes. At least three explanations are plausible for the differences between experimental and theoretical rising velocities. Weathered pellets had slightly lower experimental density than pristine pellets, as measured by density column, which indicates that environmental processing may change plastic density and introduce a systematic bias to theoretical calculations for rising/settling velocities. It is also possible that weathered pellets had more variable density values than the pristine pellets. This emphasises the importance of validating theoretical predictions for the movement and/or fate of microplastic, in this case for rising/settling velocities, with direct experimental measurements. With respect to the current study, having a complete set of experimental density measurements would have allowed reasons for the discrepancy between experimental and theoretical rising velocities to have been explained with more confidence. Another limitation of the current study is that the impact of biofilms was not investigated, as pellets were rinsed in Milli-Q water and stored at room temperature before being tested. Previous work suggests that while biofouling can increase the density of larger plastic objects in particular, causing them to sink,<sup>25</sup> spherical

microplastics above 600  $\mu\text{m}$  diameter with a density of 925  $\text{kg m}^{-3}$ , for example, low density polyethylene pellets, are unlikely to reach the density of seawater due to marine biofouling.<sup>37</sup> Results from this study suggest that density columns are a quick and easy method to measure density values. However, if lower density values were used for weathered pellets this would lead to an increase in the theoretical rising velocities and in turn their discrepancy with experimental velocities, so this cannot explain the difference in this case. Instead, the tendency for flatter (*i.e.*, typically more weathered) pellets to oscillate horizontally as they rose through the experimental rig can explain at least some of the discrepancy between experimental and theoretical rising velocities. Likewise, the fact that weathered pellets had slightly rougher surfaces, as quantified by AFM analysis, may contribute to theoretical rising velocities being higher than experimental velocities, even if roughness differences were slight. It is possible that the accuracy of calculated rising/settling velocities could be improved by modifying existing equations for heavily weathered pellets, to account for their surface properties and behaviour being different to pristine pellets.

Data displayed in Fig. 3 suggests that it is possible to distinguish between pristine low-density polyethylene and polypropylene pellets on the basis of their experimental rising velocities, since there was no overlap between the two datasets. Rising velocities for pristine low-density polyethylene pellets ranged from 4.60  $\text{cm s}^{-1}$  to 6.52  $\text{cm s}^{-1}$ , with equivalent values for polyethylene pellets from 6.19  $\text{cm s}^{-1}$  to 8.46  $\text{cm s}^{-1}$ . Indeed, distinguishing between polymers on the basis of their experimental rising/settling velocities (or by use of a density column) may be more straightforward than identifying specific polymers on the basis of spectroscopic measurements, especially when undertaking experimental work away from well-equipped laboratories, *e.g.*, when conducting fieldwork. However, experimental rising velocities for pristine high-density polyethylene pellets overlapped with values for both low-density polyethylene and polypropylene pellets, while weathered pellets had far more variable rising velocities (Fig. 3), so this approach would be most suited to spherical polymer particles with significantly different densities.

## 5. Conclusions

This study compared the experimental and theoretical rising velocities of pristine and weathered plastic production pellets (often known as nurdles or resin pellets). Surface properties were analysed using XPS and AFM. Key contributions to knowledge are as follows:

- XPS analysis revealed that the proportion of oxidised carbon species were 2.3% and 4.0% of the total carbon signal for a pristine and a weathered pellet, respectively, which is consistent with environmental processing, more specifically photochemical reactions, changing the surface chemistry of weathered pellets.
- The density of a subset of pellets was measured by density column, which was found to be a suitable analytical method for



measuring microplastic densities. Weathered pellets had slightly lower densities than pristine pellets.

- Experimental rising velocities for 140 weathered pellets varied from  $(2.36 \pm 0.01) \text{ cm s}^{-1}$  to  $(10.56 \pm 0.26) \text{ cm s}^{-1}$ , with a mean value of  $(5.79 \pm 0.06) \text{ cm s}^{-1}$ . Mean rising velocities for pristine low-density polyethylene, high-density polyethylene and polypropylene pellets were respectively  $(5.31 \pm 0.06) \text{ cm s}^{-1}$ ,  $(6.14 \pm 0.07) \text{ cm s}^{-1}$  and  $(7.42 \pm 0.08) \text{ cm s}^{-1}$ . The shape and rising velocities of pristine pellets were less variable than for weathered pellets.

- Theoretical rising velocities were consistently higher than experimental velocities for all pellet types: on average 107%, 136%, 140% and 117% of experimental values for high-density polyethylene pellets, weathered pellets, low-density polyethylene pellets and polypropylene pellets. The tendency for flatter, often more heavily weathered pellets, to oscillate as they rose explains at least some of the discrepancy between experimental and theoretical rising velocities.

- As analysed by AFM, the roughness of the pristine and weathered pellets was  $(59 \pm 11) \text{ nm}$ , and  $(74 \pm 26) \text{ nm}$  respectively. The slightly higher roughness of heavily weathered pellets may contribute to their theoretical rising velocities being less accurately predicted than for less weathered pellets.

- The study illustrates how theoretical rising and settling velocities of weathered microplastics can be overestimated. It is recommended that modelling studies which predict the environmental fate and/or movements of microplastics validate findings using experimental data.

## Conflicts of interest

There are no conflicts to declare.

## Acknowledgements

Financial support from the Engineering and Physical Sciences Research Council (EPSRC), as part of project EP/S029427/1 on *Predicting the Polymer-specific Fate of Aquatic Plastic Litter*, Research England and the University of Surrey's Strategic Priorities Funding scheme is gratefully acknowledged. NPL acknowledge funding from the UK Department of Business, Energy and Industrial Strategy through the National Measurement System programme (projects NMS/ST21). Thanks also to H&D Fitzgerald (<https://www.density.co.uk/>) for their help with the density column tests.

## References

- 1 R. Geyer, J. R. Jambeck and K. L. Law, Production, use, and fate of all plastics ever made, *Sci. Adv.*, 2017, 3(7), DOI: [10.1126/sciadv.1700782](https://doi.org/10.1126/sciadv.1700782).
- 2 GESAMP, *Sources, Fate and Effects of Microplastics in the Marine Environment: Part 2 of a Global Assessment*, 2016.
- 3 M. U. Ali, S. Lin, B. Yousaf, Q. Abbas, M. A. M. Munir, M. U. Ali, A. Rasihd, C. Zheng, X. Kuang and M. H. Wong, Environmental emission, fate and transformation of microplastics in biotic and abiotic compartments: global status, recent advances and future perspectives, *Sci. Total Environ.*, 2021, 791, 148422.
- 4 C. Wayman and H. Niemann, The fate of plastic in the ocean environment – a minireview, *Environ. Sci.: Process. Impacts*, 2021, 23, 198–212.
- 5 E. Van Seville, C. Wilcox, L. Lebreton, N. Maximenko, B. D. Hardesty, J. A. Van Franeker, M. Eriksen, D. Siegel, F. Galgani and K. L. Law, A global inventory of small floating plastic debris, *Environ. Res. Lett.*, 2015, 10, 124006.
- 6 L. Lebreton, M. Egger and B. Slat, A global mass budget for positively buoyant macroplastic debris in the ocean, *Sci. Rep.*, 2019, 9, 12922.
- 7 R. W. Obbard, S. Sadri, Y. Q. Wong, A. A. Khitun, I. Baker and R. C. Thompson, Global warming releases microplastic legacy frozen in Arctic Sea ice, *Earth's Future*, 2014, 2, 315–320.
- 8 D. K. A. Barnes, A. Walters and L. Gonçalves, Macroplastics at sea around Antarctica, *Mar. Environ. Res.*, 2010, 70, 250–252.
- 9 T. Bond, V. Ferrandiz-Mas, M. Felipe-Sotelo and E. van Seville, The occurrence and degradation of aquatic plastic litter based on polymer physicochemical properties: a review, *Crit. Rev. Environ. Sci. Technol.*, 2018, 48, 685–722.
- 10 S. C. Gall and R. C. Thompson, The impact of debris on marine life, *Mar. Pollut. Bull.*, 2014, 92, 170–179.
- 11 E. L. Teuten, J. M. Saquing, D. R. U. Knappe, M. A. Barlaz, S. Jonsson, A. Björn, S. J. Rowland, R. C. Thompson, T. S. Galloway, R. Yamashita, D. Ochi, Y. Watanuki, C. Moore, P. H. Viet, T. S. Tana, M. Prudente, R. Boonyatumanond, M. P. Zakaria, K. Akkhavong, Y. Ogata, H. Hirai, S. Iwasa, K. Mizukawa, Y. Hagino, A. Imamura, M. Saha and H. Takada, Transport and release of chemicals from plastics to the environment and to wildlife, *Philos. Trans. R. Soc. Lond. Ser. B Biol. Sci.*, 2009, 364(1526), 2027–2045.
- 12 B. Sarkar, P. D. Dissanayake, N. S. Bolan, J. Y. Dar, M. Kumar, M. N. Haque, R. Mukhopadhyay, S. Ramanayaka, J. K. Biswas, D. C. W. Tsang, J. Rinklebe and Y. S. Ok, Challenges and opportunities in sustainable management of microplastics and nanoplastics in the environment, *Environ. Res.*, 2021, 112179.
- 13 P. Bhatt, V. M. Pathak, A. R. Bagheri and M. Bilal, Microplastic contaminants in the aqueous environment, fate, toxicity consequences, and remediation strategies, *Environ. Res.*, 2021, 200, 111762.
- 14 A. Chamas, H. Moon, J. Zheng, Y. Qiu, T. Tabassum, J. H. Jang, M. Abu-Omar, S. L. Scott and S. Suh, Degradation Rates of Plastics in the Environment, *ACS Sustain. Chem. Eng.*, 2020, 8(9), 3494–3511.
- 15 B. Gewert, M. M. Plassmann and M. Macleod, Pathways for degradation of plastic polymers floating in the marine environment, *Environ. Sci.: Process. Impacts*, 2015, 17, 1513–1521.
- 16 A. L. Andrady, Microplastics in the marine environment, *Mar. Pollut. Bull.*, 2011, 62(8), 1596–1605.



- 17 P. L. Corcoran, Benthic plastic debris in marine and fresh water environments, *Environ. Sci. Process, Environ. Sci. Process. Impacts*, 2015, **17**, 1363–1369.
- 18 A. L. Andrady, The plastic in microplastics: a review, *Mar. Pollut. Bull.*, 2017, **119**(1), 12–22.
- 19 K. N. Fotopoulou and H. K. Karapanagioti, Surface properties of beached plastic pellets, *Mar. Environ. Res.*, 2012, **81**, 70–77.
- 20 D. A. Cooper and P. L. Corcoran, Effects of mechanical and chemical processes on the degradation of plastic beach debris on the island of Kauai, Hawaii, *Mar. Pollut. Bull.*, 2010, **60**(5), 650–654.
- 21 A. Turner and L. Holmes, Occurrence, distribution and characteristics of beached plastic production pellets on the island of Malta (central Mediterranean), *Mar. Pollut. Bull.*, 2011, **62**, 377–381.
- 22 P. L. Corcoran, T. Norris, T. Ceccanese, M. J. Walzak, P. A. Helm and C. H. Marvin, Hidden plastics of Lake Ontario, Canada and their potential preservation in the sediment record, *Environ. Pollut.*, 2015, **204**, 17–25.
- 23 L. A. Holmes, A. Turner and R. C. Thompson, Adsorption of trace metals to plastic resin pellets in the marine environment, *Environ. Pollut.*, 2012, **160**, 42–48.
- 24 University of Hawai'i, *Practices of Science: Making Simulated Seawater*, <https://manoa.hawaii.edu/exploringourfluidearth/physical/density-effects/density-temperature-and-salinity/practices-science-making-simulated-seawater>, accessed 21 June 2021.
- 25 D. Kaiser, N. Kowalski and J. J. Waniek, Effects of biofouling on the sinking behavior of microplastics, *Environ. Res. Lett.*, 2017, **12**, 124003.
- 26 W. E. Dietrich, Settling velocity of natural particles, *Water Resour. Res.*, 1982, **18**, 1615–1626.
- 27 N. Kowalski, A. M. Reichardt and J. J. Waniek, Sinking rates of microplastics and potential implications of their alteration by physical, biological, and chemical factors, *Mar. Pollut. Bull.*, 2016, **109**, 310–319.
- 28 M. Kooi, E. H. Van Nes, M. Scheffer and A. A. Koelmans, Ups and Downs in the Ocean: Effects of Biofouling on Vertical Transport of Microplastics, *Environ. Sci. Technol.*, 2017, **51**, 7963–7971.
- 29 P. U. Iyare, S. K. Ouki and T. Bond, Microplastics removal in wastewater treatment plants: a critical review, *Environ. Sci. Water Res. Technol.*, 2020, **6**, 2664–2675.
- 30 K. Waldschläger and H. Schüttrumpf, Effects of Particle Properties on the Settling and Rise Velocities of Microplastics in Freshwater under Laboratory Conditions, *Environ. Sci. Technol.*, 2019, **53**, 1958–1966.
- 31 K. Waldschläger, M. Born, W. Cowger, A. Gray and H. Schüttrumpf, Settling and rising velocities of environmentally weathered micro- and macroplastic particles, *Environ. Res.*, 2020, **191**, 110192.
- 32 K. Karkanorachaki, E. Syranidou and N. Kalogerakis, Sinking characteristics of microplastics in the marine environment, *Sci. Total Environ.*, 2021, **793**, 148526.
- 33 Y. Ogata, H. Takada, K. Mizukawa, H. Hirai, S. Iwasa, S. Endo, Y. Mato, M. Saha, K. Okuda, A. Nakashima, M. Murakami, N. Zurcher, R. Booyatumanondo, M. P. Zakaria, L. Q. Dung, M. Gordon, C. Míguez, S. Suzuki, C. Moore, H. K. Karapanagioti, S. Weerts, T. McClurg, E. Burres, W. Smith, M. Van Velkenburg, J. S. Lang, R. C. Lang, D. Laursen, B. Danner, N. Stewardson and R. C. Thompson, International Pellet Watch: Global monitoring of persistent organic pollutants (POPs) in coastal waters. 1. Initial phase data on PCBs, DDTs, and HCHs, *Mar. Pollut. Bull.*, 2009, **58**, 1437–1446.
- 34 C. C. Tang, H. I. Chen, P. Brimblecombe and C. L. Lee, Textural, surface and chemical properties of polyvinyl chloride particles degraded in a simulated environment, *Mar. Pollut. Bull.*, 2018, **133**, 392–401.
- 35 A. G. Shard and S. J. Spencer, Intensity calibration for monochromated Al K $\alpha$  XPS instruments using polyethylene, *Surf. Interface Anal.*, 2019, **51**, 618–626.
- 36 W. McMahon, H. A. Birdsall, G. R. Johnson, C. T. Camilli and C. T. Camilli, Degradation Studies of Polyethylene Terephthalate, *J. Chem. Eng. Data*, 1959, **4**(1), 57–79.
- 37 M. Van Melkebeke, C. Janssen and S. De Meester, Characteristics and Sinking Behavior of Typical Microplastics Including the Potential Effect of Biofouling: Implications for Remediation, *Environ. Sci. Technol.*, 2020, **54**, 8668–8680.

